Selection and Admixture in a Polytypic Aposematic Frog

Justin Yeager,^{1,2,*} Graham E. Derryberry,^{1,3} Michael J. Blum,^{1,3} and Corinne L. Richards-Zawacki^{1,4}

1. Department of Ecology and Evolutionary Biology, Tulane University, New Orleans, Louisiana 70118; 2. Biodiversidad Medio Ambiente y Salud (BIOMAS), Universidad de Las Américas, De Los Colimes esq., Quito 170125, Ecuador; 3. Department of Ecology and Evolutionary Biology, University of Tennessee, Knoxville, Tennessee 37996; 4. Smithsonian Tropical Research Institute, Panama City 0843-03092, Panama; and Department of Biological Sciences, University of Pittsburgh, Pennsylvania 15260

Submitted December 8, 2021; Accepted August 1, 2022; Electronically published January 5, 2023 Online enhancements: supplemental PDF.

ABSTRACT: Phenotypic differentiation within polytypic species is often attributed to selection, particularly when selection might be acting on a trait that serves as a signal for predator avoidance and mate choice. We evaluated this hypothesis by examining phenotypic and genotypic clines between populations of the strawberry poison frog Oophaga pumilio, a polytypic species that exhibits aposematic color pattern variation that is thought to be subject to both natural and sexual selection. Our aim was to assess the extent of admixture and to estimate the strength of selection acting on coloration across a region of Panama where monomorphic populations of distinctly colored frogs are separated by polymorphic populations containing both color variants alongside intermediately colored individuals. We detected sharp clinal transitions across the study region, which is an expected outcome of strong selection, but we also detected evidence of widespread admixture, even at sites far from the phenotypic transition zone. Additionally, genotypic and phenotypic clines were neither concordant nor coincident, and with one exception, selection coefficients estimated from cline attributes were small. These results suggest that strong selection is not required for the maintenance of phenotypic divergence within polytypic species, challenging the long-standing notion that strong selection is implicit in the evolution of warning signals.

Keywords: cline theory, phenotypic divergence, color pattern variation, Panama, poison frog, Oophaga pumilio.

Introduction

Strong selection is often identified as the most likely mechanism responsible for phenotypic variation within polytypic species (i.e., a species with two or more populations exhibiting distinct phenotypes), particularly those utilizing visual signals like aposematism (i.e., warning coloration) to mitigate predation risk (Mallet and Barton 1989). Although it is enticing to presume that strong selection results in the geographic organization of warning

signals, a growing literature suggests that other mechanisms can also give rise to rapid color pattern divergence in polytypic species (Knowles and Richards 2005; Gehara et al. 2013; Runemark et al. 2014; Yeager and Barnett 2020), even in species exhibiting aposematic coloration (Brower 1994). For example, cycles of vicariance and reconnection can result in periods of geographic isolation during which genetic drift gives rise to divergence (Knowles and Richards 2005; Runemark et al. 2010, 2014; Gehara et al. 2013). Phenotypic differentiation may also result from a combination of selective and neutral processes (e.g., Runemark et al. 2010), including sequential mechanisms like coupled drift, where differences that initially arise as a consequence of genetic drift are then maintained or amplified by selection. While evidence for mechanisms like coupled drift remains elusive, tacit elevation of strong selection over other possibilities (e.g., weak selection, neutral processes) is becoming an increasingly tenuous approach for explaining the origins and maintenance of phenotypic differentiation, even in studies of aposematic species (Tazzyman and Iwasa 2010). Thus, gaining further insight into the geographic organization of aposematism could substantively improve understanding of among-population divergence in polytypic species.

The analysis of clinal transitions (i.e., tension zones) has proven to be a particularly informative approach for characterizing the conditions that foster and maintain phenotypic variation, including the nature and strength of selection acting across phenotypically divergent populations of polytypic species (Barton and Hewitt 1985). Clinal analysis involves examining admixture proportions and the characteristics of transitions across tension zones (Barton 1979; Barton and Hewitt 1985; Barton and Gale 1993). Determining the coincidence, concordance, stability, and shape of clines can provide a basis for drawing inferences about

^{*} Corresponding author; email: yeagerjd@gmail.com.

the underlying evolutionary, ecological, and organismal conditions, ranging from the nature and strength of selection to the genetic architecture (e.g., the number of loci) underlying phenotypic traits thought to be under selection (e.g., Nadeau et al. 2014; Vestergaard et al. 2015). Work on Heliconius butterflies, widely considered to be a model study system, illustrates how clinal analysis can improve understanding of warning color pattern variation across populations within a polytypic species (e.g., Mallet and Barton 1989; Mallet et al. 1990; Blum 2002, 2008; Nadeau et al. 2014; Rosser et al. 2014). A combination of observational (e.g., Mallet 1986; Mallet et al. 1990; Blum 2002, 2008) and experimental (e.g., Mallet and Barton 1989) work indicates that wing color pattern variation within Heliconius species can be a consequence of conventional forms of selection acting in conjunction with other processes, such as dominance drive (i.e., symmetric selection on phenotypes but asymmetric selection on alleles due to differences in dominance; Mallet 1986; Blum 2002). Likewise, understanding has been gained about the relative influence of factors shaping phenotypic divergence from clinal analyses of transition zones between distinct forms of the aposematic mimic poison frog Ranitomeya imitator (Twomey et al. 2016), pointing to the possibility that further progress could be made through additional study of other polytypic dendrobatid frogs.

Like Heliconius butterflies, dendrobatid poison frogs offer exceptional opportunities for studying the basis of intraspecific phenotypic divergence (Twomey et al. 2014, 2016; Vestergaard et al. 2015). A number of parallels exist between poison frogs and Heliconius butterflies. For instance, many poison frogs are aposematic prey species that exhibit warning coloration associated with defensive traits (Saporito et al. 2009; Yeager and Barnett 2021). And like in Heliconius butterflies, Müllerian and Batesian mimicry are present in some poison frog genera. For example, phenotypically distinct comimetic species in the genus Ranitomeya often occur in sympatry (Symula et al. 2001; Yeager et al. 2012; Twomey et al. 2014). Additionally, some evidence suggests that natural selection fosters phenotypic divergence in warning coloration by promoting prezygotic isolation through immigrant inviability, where local phenotypes are favored over nonlocal phenotypes (e.g., in Dendrobates tinctorius; Noonan and Comeault 2009). Warning coloration may also be utilized in mate assessment and intrasexual conflict (Seehausen and Schluter 2004; Cummings and Crothers 2013; Yang et al. 2016, 2018). Nonetheless, questions remain about the role of selection in promoting phenotypic differentiation within polytypic species of dendrobatid frogs (Twomey et al. 2014).

The strawberry poison frog *Oophaga pumilio* serves as a particularly useful system to study the basis of phenotypic divergence within dendrobatid frogs, in part be-

cause it exhibits a geographic mosaic of phenotypes (Daly and Myers 1967) across the Bocas del Toro region of Panama, including distinct color morphs inhabiting islands belonging to the Bocas del Toro archipelago (Wang and Shaffer 2008). The remarkable color pattern diversity in O. pumilio is generally thought to have evolved through a combination of strong natural and sexual selection (Summers et al. 1997; Brown et al. 2010), but some evidence suggests otherwise. For example, predation experiments offer mixed support for natural selection acting on color pattern in O. pumilio (Hegna et al. 2013; Richards-Zawacki et al. 2013; Dreher et al. 2015; Yeager 2015), possibly because contemporary predator-mediated natural selection pressures are weak. Mate choice experiments have demonstrated that females prefer color pattern phenotypes similar to their own in a mate (Summers et al. 1999; Reynolds and Fitzpatrick 2007; Maan and Cummings 2008), but preference in polymorphic populations has been found either to be assortative or to favor a single morph (Richards-Zawacki and Cummings 2010; Yang et al. 2016). Mating preferences are additionally influenced via imprinting during maternal food provisioning (Yang et al. 2019b). Despite this, O. pumilio from allopatric populations (i.e., those that inhabit different islands) readily interbreed in captivity, producing viable offspring (Summers et al. 2004) that do not exhibit intrinsic postzygotic incompatibilities (Dugas and Richards-Zawacki 2015).

In this study, we examined patterns of clinal variation to better understand the nature and strength of selection acting on O. pumilio. We focused on the Bocas del Toro region of Panama, where populations of monomorphic red- and bluecolored O. pumilio are separated by populations composed of both red and blue phenotypes along with individuals exhibiting intermediate phenotypes (Yang et al. 2018). We compared multilocus genotypic and multiple phenotypic clines to test the hypothesis that selection on coloration drives phenotypic divergence in O. pumilio. We did so by assessing the extent and distribution of admixture as well as the slope of clinal transitions, with the expectation that narrow sigmoidal (i.e., sharp) genotypic and phenotypic transitions are indicative of strong selection (Barton and Hewitt 1985; Barton and Gale 1993). We additionally tested for cline coincidence and concordance, which are also expected outcomes of strong selection (Barton and Hewitt 1985; Barton and Gale 1993; Cummings and Crothers 2013). We drew further inferences about the importance of selection on the basis of the geographic location of clinal transitions (e.g., associations with obvious exogenous changes that could reflect differences in selective pressures), and we estimated the strength of selection according to the structure of genotypic and phenotypic clines. This allowed us to derive further insights about

the conditions underlying phenotypic differentiation in O. pumilio, providing new perspectives on whether and how selection contributes to the evolution of polytypic species.

Material and Methods

Study Area and Populations

Sites were sampled across a transect in the Bocas del Toro region (fig. 1) that spanned a transition zone from monomorphic red populations on the mainland and San Cristobal Island to monomorphic blue populations on the southern Aguacate peninsula (hereafter referred to as the "Aguacate transition zone"). Populations of frogs exhibiting a mixture of phenotypes, ranging from red to intermediate (brown) to blue, were found at intervening locations across the northern part of the Aguacate peninsula (fig. 1).

Although the ancestry of the study populations remains unresolved, prior work suggests that the diversity of Oophaga pumilio phenotypes in the archipelago and adjacent mainland regions arose from a widely distributed ancestral red-bodied phenotype (Wang and Shaffer 2008). Repeated colonization of the archipelago may have fostered evolutionary diversification (Wang and Shaffer 2008), but mitochondrial DNA sequence variation (Hagemann and Pröhl 2007) indicates that there are only three main lineages of O. pumilio: a northern (Costa Rica), a southern (Bocas del Toro, Panama), and an eastern (Isla Escudo de Veraguas, Panama) lineage. The northern and southern lineages of O. pumilio appear to transition north of the Aguacate peninsula, although some individuals from two mainland populations and San Cristobal Island farther south exhibit genotypes that are similar to the northern lineage (Hauswaldt et al. 2011). There is also evidence (e.g., amplified fragment length polymorphisms; Rudh et al. 2007) that Panamanian populations from Cerro Brujo on the Aguacate peninsula and nearby San Cristobal Island form a genetic cluster that is distinct from other populations within the archipelago. These divisions suggest that the northern and southern lineages diverged in allopatry as a result of a vicariant event, whereas the contemporary admixed population distributions are the result of secondary contact (Hauswaldt et al. 2011).

Specimen Collections

We collected toe-clip tissue samples of O. pumilio from monomorphic and polymorphic areas across the Aguacate transition zone and from reference populations outside the zone. We collected tissues from a total of 491 individuals from 30 locations (fig. 1; table 1) between June 2009 and December 2012. We collected samples from 16-22 individuals from each of 14 locations in the Aguacate transition zone where frogs are polymorphic, with collection sites spaced ≥250 m apart. We sampled individuals from monomorphic red populations at six locations (three near Almirante, three on Isla San Cristobal) in close proximity to the polymorphic populations. Likewise, we sampled individuals from six monomorphic blue populations across the southern part of the Aguacate peninsula (fig. 1). To allow for broader comparisons, we also sampled three populations that exhibit markedly different color patterns from those in and proximate to the transition zone (fig. 1; site 23: blue/green; sites 24 and 25: black/white). We preserved tissue samples in a salt-saturated dimethyl sulfoxide (DMSO) and ethylenediaminetetraacetic acid (EDTA) solution and stored them at room temperature prior to DNA extraction.

Phenotypic Trait Measurements

We characterized dorsal and ventral coloration to assess the nature of phenotypic variation across the study area (fig. 1). Although the extent of dorsal black spotting differed among individuals, all exhibited a uniform background coloration, which spanned a continuum from red to intermediate (i.e., brown) to blue across the Aguacate transition zone (fig. 1). Considering this, we quantified dorsal phenotype by eye at the time of capture using a scale of 0 to 4 (0 = blue; 1 = blue/brown; 2 = brown; 3 = red/brown; 4 = red). Unlike dorsal coloration, we did not detect intermediate brown ventral coloration. Frogs from the transition zone exhibited either a single uniform ventral color (red or blue) or exhibited a mottled venter of red and blue patches. We therefore used a different scale to score the proportional composition of red and blue ventral coloration: 0 = entirely blue; 1 = 75% blue, 25% red; 2 = 75% blue50% blue, 50% red; 3 = 75% red, 25% blue; 4 = entirely red. The utility of this type of "by-eye" phenotypic categorization for this population has been supported by comparisons with more quantitative analyses of standardized color photographs (Dugas et al. 2015; Yang et al. 2019a). We confirmed this for our study by drawing comparisons to composite scores based on color photographs on a standardized background (Rite in the Rain paper) for a subset of frogs from monomorphic and polymorphic populations (n = 277; table 1). As both approaches yielded quantitatively and qualitatively similar results (table 2; supplemental PDF), we used the larger data set of categorical by-eye scores to characterize dorsal and ventral phenotype and to compare phenotypic to genotypic variation across the transition zone. In all subsequent analyses, we considered each body surface as a separate trait because dorsal coloration is thought to be under sexual and natural selection whereas ventral coloration is thought to be under

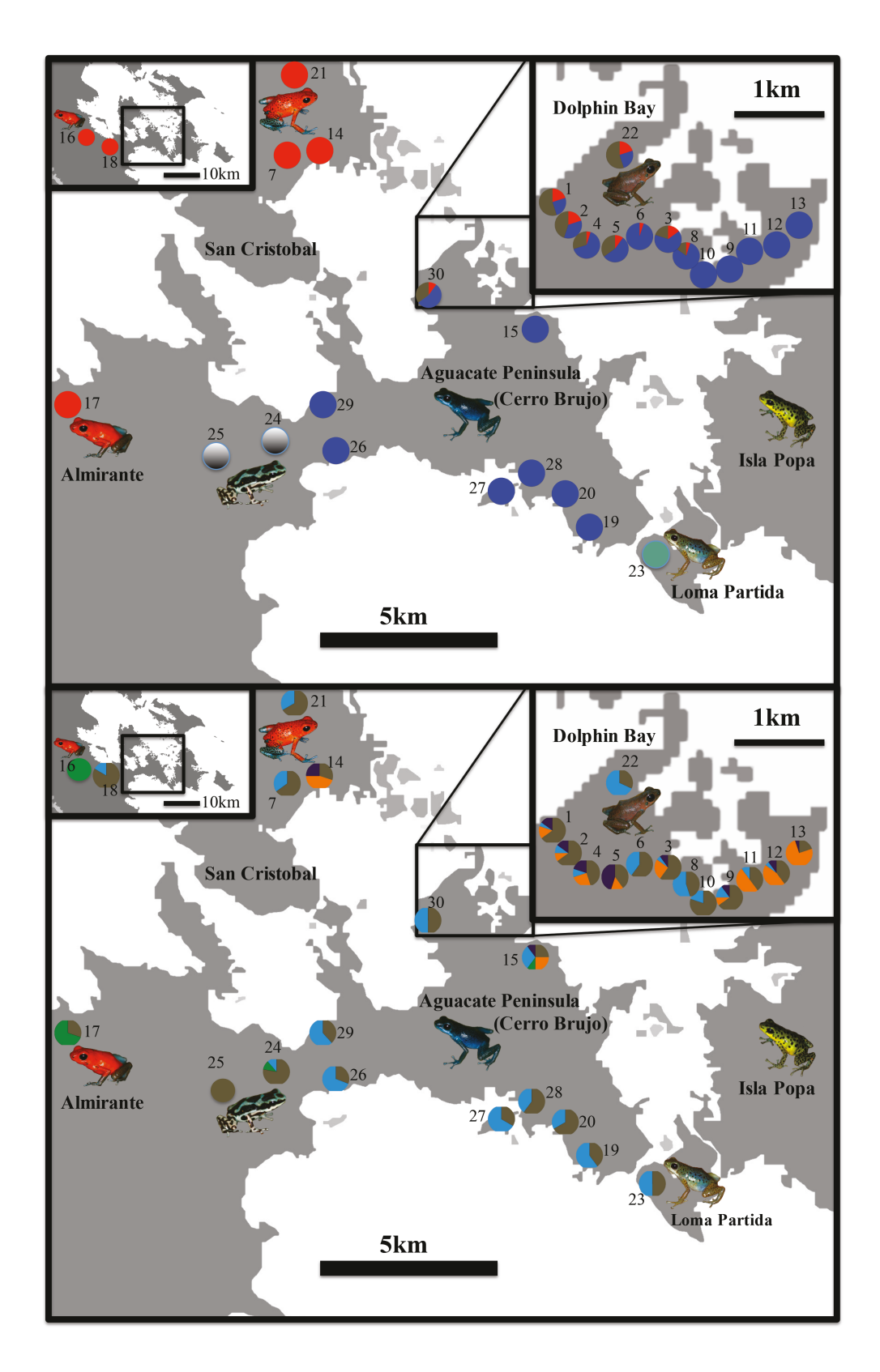


Figure 1: Maps of sampled locations showing phenotypic (top) and genotypic (bottom) transitions. Pie charts show the relative frequencies of frog coloration (top; determined using red, blue, and intermediate categorical phenotype scores of 1–3, binned for simplicity) and genotype assignments (bottom; K=4: blue, purple, orange, and green) at each locality. Brown color indicates intermediate morphs (representative photo in the top right inset) or admixed individuals (bottom). The top left inset shows the study area within the Bocas del Toro archipelago and adjacent mainland; the top right inset shows sampling along the Aguacate transition zone in the vicinity of Dolphin Bay. Although excluded from clinal analyses, adjacent distinctly colored populations (23: blue/green; 24, 25: black/white) are included for reference.

Table 1: Number of Oophaga pumilio sampled (N) from monomorphic and polymorphic populations in Bocas del Toro, Panama, and summary statistics for genetic diversity

						No.			Dorsal			Ventral		
Locality	N	$N_{ m MSAT}$	$N_{ m DRGB}$	$N_{ m VRGB}$	Distance, km	alleles	$H_{\rm O}$	$H_{\scriptscriptstyle m E}$	Blue	Inter.	Red	Blue	Inter.	Red
1	20	20	20	20	7.040	17	.846	.908	0	15	5	11	9	0
2	20	20	20	20	7.314	17	.829	.907	4	11	5	16	3	0
3	20	20	20	20	8.011	17	.818	.922	7	11	2	18	2	0
4	20	20	20	20	7.610	18	.806	.913	4	13	3	18	2	0
5	20	20	20	20	7.794	19	.828	.920	7	10	3	17	3	0
6	20	20	20	20	8.104	16	.714	.869	13	6	1	20	0	0
7	20	20	10	10	3.208	13	.770	.862	0	0	20	0	0	0
8	20	20	19	19	8.250	14	.795	.871	11	8	1	0	0	0
9	20	20	20	20	8.613	15	.781	.853	15	5	0	0	0	0
10	20	20	20	20	8.814	18	.788	.896	19	1	0	0	0	0
11	20	20	0	0	8.734	19	.846	.927	20	0	0	0	0	0
12	20	20	0	0	8.752	16	.754	.901	20	0	0	0	0	0
13	20	20	0	0	8.867	16	.854	.913	20	0	0	0	0	0
14	20	20	20	20	2.953	18	.833	.922	0	0	20	0	0	0
15	20	20	9	9	11.718	16	.801	.901	20	0	0	0	0	0
16	20	20	20	20		8	.888	.752						
17	40	40	39	39		14	.864	.828						
18	12	12	0	0		10	.749	.847						
19	5	5	0	0	15.429	6	.875	.876	5	0	0	0	0	0
20	3	3	0	0	14.939	5	.861	.906	3	0	0	0	0	0
21	12	12	0	0	.000	11	.824	.874	0	0	12	1	1	8
22	22	22	0	0	6.987	14	.779	.846	7	8	7	0	0	0
23	6	6	0	0	16.520	6	.778	.838	6	0	0	0	0	0
24	9	9	0	0		10	.828	.892	0	0	0	0	0	0
25	3	3	0	0		4	.806	.839	0	0	0	0	0	0
26	13	13	0	0	11.658	11	.808	.894	13	0	0	0	0	0
27	12	12	0	0	13.324	10	.771	.873	12	0	0	0	0	0
28	5	5	0	0	13.518	6	.833	.844	5	0	0	0	0	0
29	13	13	0	0	10.461	10	.833	.868	13	0	0	0	0	0
30	16	16	0	0	7.486	11	.719	.834	4	10	2	0	0	0

Note: Categorical dorsal and ventral phenotypic scores were recorded for all individuals. The NMSAT column refers to the number of frogs used in genotypic analyses, and the NDRGB and NVRGB columns show the number of frogs for which standardized color photographs of the dorsum and venter, respectively, were available for composite RGB analyses (supplemental PDF). Distance refers to the linear distance (km) from the northernmost Isla San Cristobal population (location 21), which was used to anchor cline analyses. Almirante populations were omitted from cline analyses. Locality data were intentionally omitted to discourage illegal collection. $H_{\rm E}={
m expected}$ heterozygosity; $H_{\rm O}={
m observed}$ heterozygosity.

only sexual selection (Maan and Cummings 2008; Cummings and Crothers 2013).

Microsatellite Genotyping

We genotyped all 491 individuals (fig. 1; table 1) at 12 highly variable microsatellite markers to estimate clinal variation at putatively neutral loci. We extracted genomic DNA from toe clippings using the Qiagen DNeasy Blood and Tissue kit (Qiagen, Valencia, CA) following the protocol for animal tissue (https://www.qiagen.com/us/resources /download.aspx?id = 68f29296-5a9f-40fa-8b3d-1c148d0b 3030&lang = en; accessed August 4, 2021). We then genotyped each individual at the following loci using primers

that were developed for O. pumilio: Dpum92, Dpum44, and Dpum110 (Wang and Summers 2009) as well as Oop O1, Oop G5, Oop C11, Oop E3, Oop F1, Oop B8, Oop_B9, Oop_C3, and Oop_D4 (Hauswaldt et al. 2009). Polymerase chain reaction (PCR) amplifications were done in 10- μ L reaction volumes that included 4 μ L of GoTaq Green Master mix (Promega, Madison, WI) and 0.5 μL of a 10-μM solution containing each of the forward and reverse primers. In reactions with the Hauswaldt et al. (2009) primers, we used 1 μ L of undiluted genomic DNA, whereas reactions using the Wang and Summers (2009) primers contained 1.5 μ L of undiluted genomic DNA plus 1 μ L of 2.5 mM MgCl₂. Thermal cycling conditions followed Hauswaldt et al. (2009) for the Oop primers except that

Table 2: Summary of phenotypic and genotypic cline models, including estimated centers, widths, and Akaike's information criterior
(AIC) and likelihood values

	Cline 1	model			Selection coefficient				
	selected		Estima		A.	R.	О.		
Cline	Scaling	Tails	Center	Width	Loglik	AIC	femoralis	imitator	pumilio
Dorsal	Free	None	7.52 (7.46-7.55)	.86 (.8192)	745.51	-1,476.75	.0027	.0778	.0008
Ventral	Free	None	7.25 (7.12–7.26)	.45 (.4555)	132.75	-250.98	.0038	.1076	.0011
Genotypic	Free	None	9.56 (8.87-10.45)	.08 (<.0110)	-173.05	360.10	.0089	.2552	.0027
Ventral PC1	Free	None	5.02 (4.89-5.37)	2.61 (1.48-2.72)	-921.23	1,856.47	.0016	.0447	.0005
Dorsal PC1	Fixed	Both	6.84 (6.61-6.98)	2.87 (2.46-3.53)	-891.28	1,796.55	.0015	.0426	.0004

Note: Cline scaling and tails refer to elements of the shape of clines. All distance measures are presented in kilometers starting from the anchor location on Isla San Cristobal (location 21; fig. 1). Selection coefficient estimates are reported for low-dispersal and high-dispersal distance estimates. Cline results in bold-face type correspond to those illustrated in figure 3, and those not in boldface type are shown in figure S2. CI = confidence interval; loglik = log likelihood.

we used an annealing temperature of 55°C. Reaction conditions followed Wang and Summers (2009) for the Dpum primers except that we used an annealing temperature of 52°C for Dpum44 and of 60°C for Dpum110. We characterized PCR products on an ABI 3730xl (Applied Biosystems, Forest City, CA) and scored them using GeneMarker (ver. 1.90; Softgenetics, State College, PA) against a LIZ 500 size standard (Applied Biosystems, Waltham, MA).

Analysis of Genetic Differentiation and Admixture

We characterized patterns of microsatellite allelic variation to infer the extent of genetic differentiation and admixture across the Aguacate transition zone. We tested for Hardy-Weinberg equilibrium, calculated allele frequencies between sampled populations, and estimated observed (H_0) and expected (H_E) heterozygosity in Arlequin (ver. 3.5; Excoffier et al. 2005; table 1). We also calculated pairwise $F_{\rm ST}$ values to gain greater perspective on the nature and degree of genetic variation among the sampled populations. We used STRUCTURE (ver. 2.3.4; Pritchard et al. 2000) to iteratively explore the possibility of hierarchical genetic structure according to geography and phenotype as well as to determine the most appropriate "parental" red population to include in clinal analyses. This involved running an initial set of five independent analyses of the full data set (which included both potential parental monomorphic red populations from Almirante and San Cristobal) with K values ranging from 1 to 15 and with 30,000 burn-in runs and 3,000,000 data collection runs. To better assess the nature of genotypic clustering among individuals exhibiting a red phenotype in the study area, we then ran two separate analyses of reduced data sets that included either mainland (Almirante) or insular (San Cristobal) red populations with samples from all other locations. For each of these data subsets, we performed five replicate analyses, each time allowing K to vary from 1 to 5, with 30,000 burn-in runs and

3,000,000 data collection runs. Results of all runs were visualized with the main pipeline from CLUMPAK (http://clumpak.tau.ac.il/index.html) to assess population structure and the extent of admixture within individuals and populations.

Clinal Variation in Genotypic and Phenotypic Traits

We used the R (ver. 3.6.0; R Core Team 2020) package HZAR (Derryberry et al. 2014) to describe clinal transitions in the frequency of multilocus genotypes, dorsal color phenotypes, and ventral color phenotypes across the Aguacate transition zone. We generated linear distances in HZAR using monomorphic red and monomorphic blue populations as the termini of the multilocus genotypic and phenotypic clines. We then built genotypic clines using average admixture frequencies from the STRUCTURE analyses that revealed the most likely number of genetic clusters within the sampled populations. Phenotypic clines were built using categorical scores for dorsal and ventral coloration. For comparison, we also built clines using composite scores based on principle component analysis (PCA) and K-means clustering of RGB values extracted from color photographs (supplemental PDF).

HZAR fits cline models to both molecular and phenotypic traits utilizing Metropolis-Hastings Monte Carlo Markov chain (MCMC) algorithms by applying likelihood function tests for alternative cline model shapes. The Autofit feature in HZAR automates model selection between 10 quantitative trait model options for genotypic and phenotypic clines that vary in scaling (fixed, free, and none) and tail (left, right, mirror, both, and none) options to describe the shape of clinal transitions using Akaike's information criterion (AIC; Akaike 1973). Although the majority of the transition within a trait usually occurs over the width of the cline, some transitions can continue past the width into the tails (i.e., approaching putative monomorphic populations),

which can indicate a breakdown in the strength of selection. "Left" and "right" tail models indicate that gene flow is higher in the direction of one tail than predicted by cline width, whereas "mirror" tail models have identical tail shape. The "both" tail model refers to two independent tail shapes, and the "none" tail model assumes that tails do not differ from the sigmoidal transition cline. Maximum likelihood cline profiles were used to select the cline model shape, and 95% confidence intervals and likelihood profiles were used to assess coincidence and concordance between genotypic and multiple phenotypic clines.

We tested model fits against the null model of no change across the transect. We accepted models with AIC scores within two units of the lowest AIC value (AIC = $-2(\log \text{Lik}) + 2K$). We then generated cline center and width support estimates in HZAR from the set of MCMC clines within two log-likelihood units of the maximum likelihood. We assessed cline concordance and coincidence between traits (i.e., genotype, dorsal phenotype, and ventral phenotype) by comparing relative AIC values (Δ AIC relative to the minimum AIC) of the likelihood profile. If the cline models selected for each given value differed by ≥2 AIC values, then those clines were classified as noncoincident for cline centers or discordant for cline widths (Burnham and Anderson 2002; Anderson 2008).

Selection Coefficients

We estimated the strength of selection in maintaining clinal transitions by calculating the selection coefficient (s) from the structure of each of the genotypic and phenotypic clines, where

$$s = \frac{8\sigma^2}{\sqrt{w}}.$$

Following Barton and Hewitt (1985), this estimation takes into account the width of a cline (w) as well as linear intergenerational dispersal distances (σ^2). Because little is known about intergenerational dispersal in poison frogs in general, we used values from two related poison frogs representing low and high dispersal estimates, which almost certainly bracket the intergenerational dispersal distance of O. pumilio: Allobates femoralis, which has an average annual adult dispersal of 17.8 m (Ringler et al. 2009); and Ranitomeya imitator, a species with a more similar natural history for which a generational dispersal of 97 m has been estimated (for an explanation of the derivation of this estimate, see the supplemental materials for Twomey et al. 2014). For further comparison, we also used an average annual adult dispersal value of 9.74 m estimated from a mark-recapture study of adult O. pumilio (M. Dugas, unpublished data), keeping in mind that sexual maturity in O. pumilio takes approximately one year to

achieve (Yang et al. 2019b), during which time juveniles likely disperse from natal territories.

Results

Genetic Population Structure and Relationships

Significant pairwise F_{ST} values ranging from 0.02 to 0.11 were recovered between geographically proximate populations exhibiting distinct color phenotypes like the mainland monomorphic red (16-18) and nearby black/white (24, 25) populations (fig. 1). Likewise, pairwise F_{ST} values ranged from 0.03 to 0.11 between phenotypically similar but geographically distant populations, such as the monomorphic red populations on the mainland (16-18) and San Cristobal (7, 14, 21; fig. 1). A similar range of pairwise $F_{\rm ST}$ values were recovered in comparisons of monomorphic red and blue populations that served as anchors in clinal analyses.

STRUCTURE runs revealed that the most likely number of genetic clusters (*K*) supported by the full data set is two, roughly separating individuals and populations according to dominant dorsal color phenotype. The STRUCTURE runs including only one of the putative parental red populations (respectively) indicated that the most likely number of genetic clusters (K) supported in each of the two data subsets was four, and the insular San Cristobal monomorphic red populations were identified as the most genetically similar to the populations in the polymorphic region on the Aguacate peninsula. Accordingly, the San Cristobal populations were included in the analysis of a reduced data set encompassing individuals from the transition zone along with blue, black/white, and blue/green populations in the study area. The San Cristobal populations also were used to anchor cline analyses.

Genotype-Phenotype Admixture within Individuals and Populations

STRUCTURE analyses revealed evidence of genotypephenotype discordance, where genetic assignments were often dissimilar among frogs exhibiting similar phenotypes (figs. 1, 2). STRUCTURE analyses also recovered evidence of individual and population-level admixture across the study area (figs. 1, 2). Individual-level admixture was most evident across the phenotypic transition zone, including in the red monomorphic Isla San Cristobal populations, which suggests that our sampling did not capture the north-northwestern end of clinal transitions across the study area. In comparison, evidence of little to no admixture in the terminal monomorphic blue populations indicates that we did capture the south-southeastern end of the clinal transitions (fig. 2). Likewise, we detected evidence of individual and population-level admixture at sites

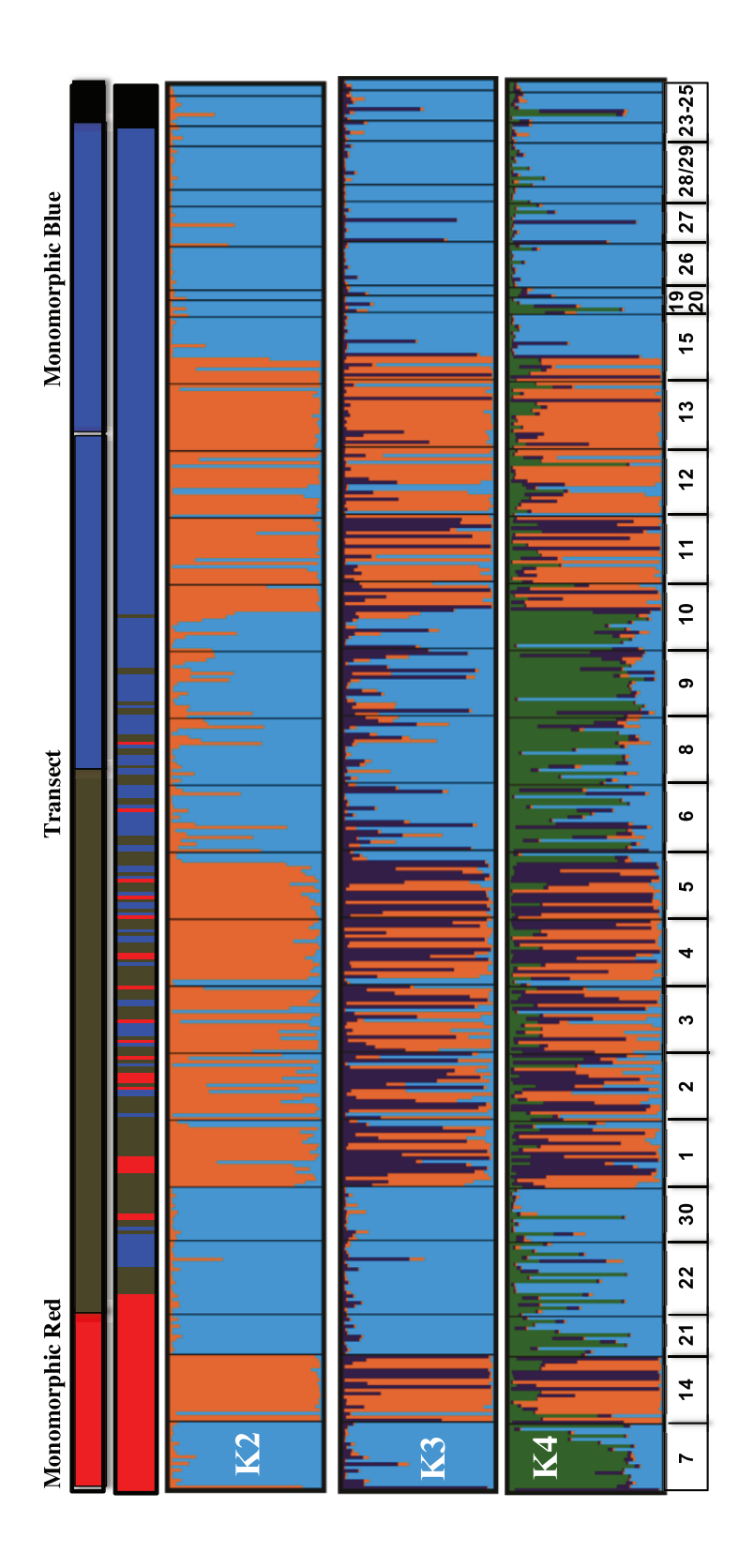


Figure 2: Results of STRUCTURE assignments averaged over five independent analyses of the Isla San Cristobal-anchored reduced data set showing genetic clustering across the study transect. *K* values of 2–4 are shown in separate panels. Information provided for reference includes the sample locations (numbers at the bottom), population-wide dorsal phenotype classification (top bar), and individual categorical dorsal phenotype scores (middle bar), where red indicates the red phenotype (categorical score of 4), brown indicates the intermediate phenotype (categorical score of 1–3), blue indicates the blue phenotype (categorical score of 1–3), blue indicates the blue phenotype (categorical score of 1–3).

located some distance away from the zone (fig. 2). Some individuals in monomorphic blue populations, however, exhibited admixed genotypic assignments drawing from three genetic clusters according to STRUCTURE runs from the reduced data set with assignments at K = 4 (figs. 1, 2). Patterns of admixture with cluster assignments at K = 2were similar to cluster assignments at K = 4. For example, signatures of admixture at K = 2 were found in monomorphic red populations as well as monomorphic blue populations. Populations within the phenotypic transition region also exhibited variable levels of admixture with assignments to one or the other cluster as well as signatures of within-population admixture.

Genotypic and Phenotypic Clinal Variation

Hereafter we focus on genotypic clines and phenotypic clines generated from categorical scoring of dorsal and ventral coloration. Clinal analyses of composite scores from PCA and K-means clustering of RGB values derived from photographs yielded nearly identical results (supplemental PDF). The cline reflecting multilocus genotypic variation exhibited a steep transition with a width of 0.08 km (<0.01-0.10 km) and an estimated center of 9.56 km (8.87-10.45 km) from the transect terminus (table 2). The genotypic cline exhibited no difference in sigmoidal shape past the estimated width of the cline (i.e., into the tails), and the tail shape on both sides of the transition was symmetrical although not identical. The dorsal and ventral phenotypic clines also exhibited steep transitions (table 2; fig. 3). Clines generated from categorical phenotypic scores exhibited widths of 0.86 km (0.81-0.92 km) and 0.45 km (0.45-0.55 km), with estimated centers located at 7.52 km (7.46-7.55 km) and 7.25 km (7.12-7.26 km) from the transect terminus, respectively (table 2; fig. 3). Similar to the genotypic cline, the shapes of the tails did not depart from a sigmoidal transition.

Comparison of Genotype and Phenotypic Clines

The dorsal and ventral phenotypic clines were not coincident or concordant (fig. 3; fig. S2). We also found that the genotypic cline was not coincident or concordant with any of the phenotypic clines (table 2; figure 3). The genotypic cline was offset from and narrower than all of the phenotypic clines.

Estimation of Selection

We recovered lower selection coefficient values for phenotypic clines than the genotypic cline. Selection coefficients derived from the categorical dorsal phenotype cline were 0.003, 0.078, and 0.001 based on adult dispersal distance estimates derived from Allobates femoralis, Ranitomeya imitator, and Oophaga pumilio, respectively. Selection coefficients derived from the categorical ventral phenotype cline were 0.004, 0.108, and 0.001, respectively (table 2), and selection coefficients derived from the genotypic cline were estimated as 0.009, 0.255, and 0.003, respectively.

Discussion

We examined naturally occurring genotypic and phenotypic clinal variation in the strawberry poison frog Oophaga pumilio to gain further insight into the strength of selection acting on a polytypic species displaying aposematic coloration. We did not find patterns of clinal concordance and coincidence that would be expected under conditions of strong selection acting on an adaptive trait such as warning coloration (Barton and Hewitt 1985; Barton and Gale 1993). Rather, we found that the estimated genotypic cline across the Aguacate transition zone is displaced from phenotypic clines. We also found that the estimated genotypic transition is much sharper than phenotypic transitions, further indicating that genetic boundaries among color morphs are not solely a reflection of selection-driven phenotypic differentiation. Selection coefficient estimates were largely consistent with inferences derived from the shape and location of genotypic and phenotypic clinal transitions. With one exception (s = 0.2552 for the genotypic cline, assuming high dispersal), selection coefficients estimated from the structure of phenotypic and genotypic clines were modest to remarkably small (s = 0.0027-0.1076) for O. pumilio, particularly in comparison to coefficients estimated for other polytypic aposematic species like Heliconius butterflies (s = 0.21-0.64; Benson 1972; Mallet 1986; Mallet et al. 1990; Blum 2002, 2008) that exhibit color pattern variation shaped by strong natural and sexual selection (Mallet and Barton 1989; Kapan 2001).

The estimated cline widths for O. pumilio were narrower than what would be expected under conditions of neutral diffusion (Endler 1977), indicating that constraints limit the diffusion of alleles and phenotypic traits across the Aguacate transition zone. Assuming that the most recent contact between Isla San Cristobal and the mainland occurred approximately 1,000 years ago (Anderson and Handley 2002) and that dispersal in O. pumilio is comparable to closely related poison frogs (Ringler et al. 2009; Twomey et al. 2014; M. Dugas, unpublished data), neutral diffusion would yield cline widths of 1.41-7.7 km. Evidence of steeper clines suggests that selection, limited dispersal, or a combination thereof is shaping transitions across the geographic mosaic of aposematic polytypism in O. pumilio (Barton and Hewitt 1985; Barton and Gale

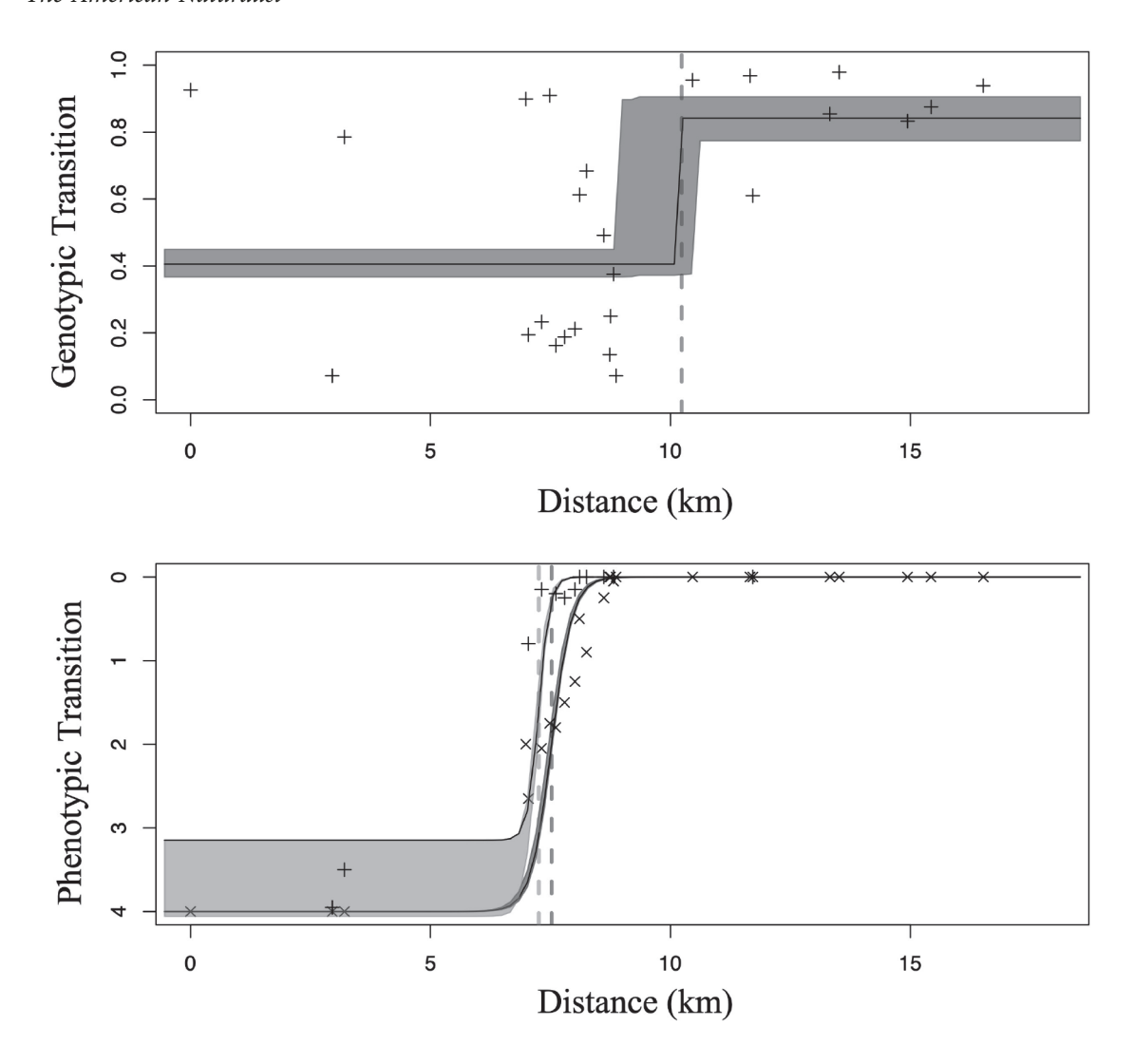


Figure 3: Estimated cline transitions for genotypic assignments generated from K = 4 STRUCTURE runs (top) and categorical phenotypic scores (bottom), noting the cline centers (dashed vertical lines) and widths for dorsal (dark gray) and ventral (light gray) phenotypic transitions. Population trait averages are represented by a plus sign for genotypes (top), by a plus sign for ventral phenotypes (bottom), and by a cross for dorsal phenotype (bottom). The left side and terminus of the clines refer to Isla San Cristobal populations 7, 14, and 21. The right side and terminus of the clines refer to populations 19 and 20 on the Aguacate Peninsula.

1993). Strong natural selection is often considered to be the most parsimonious explanation of variation in aposematic warning coloration exhibited by poison frogs (Noonan and Comeault 2009), but our findings buoy evidence from prior studies of *O. pumilio* indicating otherwise (Richards-Zawacki and Cummings 2010; Gehara et al. 2013; Dreher et al. 2015).

Several lines of reasoning point to limited dispersal being a key factor shaping clinal transitions across the Aguacate peninsula. For example, *O. pumilio* maintain small, well-defended territories (Pröhl and Berke 2001), and although intergenerational (i.e., juvenile and adult) dispersal distances are not known for *O. pumilio*, adult dispersal distances appear to be limited (M. Dugas, unpublished data).

Likewise, other closely related poison frogs exhibit relatively small adult dispersal distances (Ringler et al. 2009; Twomey et al. 2014). Additional support for the potential importance of limited dispersal can be distilled from comparisons to other notable transition zones. For instance, clines across transition zones of more vagile species in Panama are much broader (i.e., by one to two orders of magnitude), including clines in traits that are known to be under selection, such as coloration in *Heliconius* butterflies and *Manacus* birds (Mallet 1986; Brumfield et al. 2001; Blum 2002). A hybrid zone in Europe between *Bombina* toads, which exhibit much wider clines (~6 km; Szymura 1993) than those of *O. pumilio*, offers an additional point of comparison, as *Bombina* toads are much more vagile than

dendrobatids (e.g., Bombina exhibit intergenerational dispersal distances of ~430 m). Additional study of O. pumilio dispersal, particularly during the juvenile life stage, is thus warranted to further understand the evolution of polytypic differentiation.

Some evidence indicates that sexual selection may be acting in combination with limited dispersal to sharpen clinal transitions (Summers et al. 1999; Reynolds and Fitzpatrick 2007; Maan and Cummings 2008; Richards-Zawacki and Cummings 2010). This inference is supported by the estimated selection coefficients suggesting that selection is a weak to moderate force acting on O. pumilio. It is also consistent with inferences about the strength of natural and sexual selection derived from experimental studies of O. pumilio conducted in Bocas del Toro and elsewhere (Hegna et al. 2013; Richards-Zawacki et al. 2013; Dreher et al. 2015; Yeager 2015). For instance, several predation experiments did not find evidence of strong natural selection acting on coloration, where predator attack frequencies were low and the frequencies of attack did not differ among O. pumilio phenotypes (Hegna et al. 2013; Richards-Zawacki et al. 2013; Dreher et al. 2015; Yeager 2015). Similarly, studies examining sexual selection found evidence of weak color-based female preferences (Yang et al. 2016) and male aggressive biases (Yang et al. 2018) among wild individuals from the study area. On the other hand, captive frogs do exhibit color assortative preferences (Yang et al. 2019b) and color assortative mating has been detected in one population from the Aguacate transition zone (Yang et al. 2019a). Red and yellow frogs in the only other well-studied polymorphic zone (located on the island of Bastimentos) also appear to exhibit strong assortative mate preference but not asymmetric mate choice (Richards-Zawacki and Cummings 2010; Richards-Zawacki et al. 2012). Greater insight might be gained from drawing comparisons to other transition zones, as illustrated in a recent study of three transition zones between distinct forms of the mimic poison frog Ranitomeya imitator that revealed evidence of variation in the relative influence of factors shaping phenotypic divergence (Twomey et al. 2016).

Sexual selection could possibly be contributing to phenotypic divergence as a consequence of coupled drift. In a model of coupled drift based on O. pumilio, divergence in phenotypes is predicted to initially arise as a consequence of drift, after which selection via female mate choice maintains or increases phenotypic divergence between populations (Tazzyman and Iwasa 2010). Notably, a comparable outcome would be expected to arise from learned mate choice (Yang et al. 2019b). Pedigree analyses of wild populations (Richards-Zawacki et al. 2012) coupled with further observations of the mating patterns of wild frogs (Yang et al. 2019a) could clarify the extent to which sexual selection (Richards-Zawacki et al. 2012; Yang et al. 2019b) or coupled drift (Tazzyman and Iwasa 2010) drives divergence in O. pumilio.

Consideration of cline widths alongside other attributes bolsters the inference that selection is probably not the only or most important factor underlying phenotypic divergence within O. pumilio. For example, evidence of steep clines is consistent with a scenario of geographic separation caused by sea level rise, which could have resulted in secondary contact following periods of vicariant isolation (Gehara et al. 2013). While this would help explain why the present location of the cline centers is at or near the Aguacate shoreline, evidence of clinal discordance and incongruency does not align with expected outcomes of secondary contact (Barton and Hewitt 1985; Barton and Gale 1993). Steep clines also can be associated with ecological discontinuities that inhibit gene flow between ecologically divergent populations (Barton and Hewitt 1985; Barton and Gale 1993; Jiggins et al. 1997; McMillan et al. 1997; Arias et al. 2008; Blum 2008), but this scenario does not seem plausible, as the Aguacate transition zone in O. pumilio crosses a short geographic distance that does not correspond to an obvious ecological gradient. Rather, the clines may have been drawn to the Aguacate shoreline due to density troughs (i.e., where population densities are at a minimum) in unsuitable coastal habitats like open water, mangroves, or brackish marshes (Barton and Hewitt 1985; Barton and Gale 1993). Comparing population densities in and around the estimated cline centers could offer a basis for testing this hypothesis.

Evidence of weak selection and cline displacement suggests that genotypic and phenotypic clines at color pattern boundaries in O. pumilio may be unstable and prone to movement. While the observed cline transition shapes were steep, indicating that sharp genotypic and phenotypic segregation occurs over small geographic distances, we nonetheless found that the center of the genotypic cline is displaced into the geographic region dominated by frogs exhibiting a monomorphic blue phenotype. This indicates that "red frog" genotypes have introgressed into blue populations. Displacement and introgression can be due to greater permeability of neutral loci and traits (e.g., microsatellite loci) across contact zones, but the observed asymmetry across the Aguacate transition zone suggests that other factors may be structuring gene flow among neighboring populations. It is possible, for example, that the observed pattern is a reflection of genetic asymmetries, such as dominance drive (Mallet 1986; Blum 2002), or that red frog genomic attributes confer a selective advantage, perhaps reflected in female preferences for red coloration (Yang et al. 2016). If so, then the genotypic cline could be highly mobile (e.g., Blum 2002; Ward et al. 2012; Glotzbecker et al. 2016), where elements of the red frog genome would be expected to introgress deeper into the Aguacate peninsula, resulting in greater genotype-phenotype discordance over time.

While our study falls short of identifying the specific mechanism(s) underlying rapid color pattern divergence in O. pumilio, to our knowledge it is the first to offer evidence of weak selection alongside genotypic and phenotypic clinal discordance in an aposematic species. Further work could bolster our findings, but it could also show that we have underestimated the strength of selection acting on color pattern variation in O. pumilio. It is possible, for example, that weak selection coefficients represent the balance of agonistic interactions or opposing selection pressures (e.g., sexual selection acting in opposition to natural selection). It is also possible that our estimates do not reflect other forms of selection, such as episodic bouts that generate or maintain divergence. Nonetheless, our findings challenge prevailing arguments by indicating that natural selection is likely just one among several factors contributing to aposematic color variation in poison frogs like O. pumilio, underscoring the value of employing complementary approaches to infer the origins and outcomes of phenotypic divergence in polytypic species.

Acknowledgments

This work was supported by grants from the National Science Foundation (award 1146370) and the Louisiana Board of Regents (EPSCoR LINK program) to C.L.R.-Z. and a Smithsonian Tropical Research Institute (STRI) Short-Term Fellowship awarded to J.Y.; during revisions, J.Y. was also supported by Universidad de las Américas (UDLA) grant FGE.JY.22.01. We are grateful to P. Gondola and G. Jacome as well as other STRI staff in Bocas del Toro for logistical support. We are deeply grateful to E. Derryberry for assistance with data archiving and code submission. We would also like to thank B. Noonan and J. Karubian for thoughtful comments on early drafts. The Panamanian National Authority (ANAM) and the Institutional Animal Use and Care Committees at STRI and Tulane University provided permission and approval for this work.

Statement of Authorship

J.Y., M.J.B., and C.L.R.-Z. designed the experiment; J.Y. and C.L.R.-Z. secured funding for the study; J.Y. sampled frogs; J.Y., G.E.D. (code writer), and M.J.B. conducted analyses; and J.Y. and M.J.B. wrote the manuscript with significant contributions from all authors.

Data and Code Availability

Data and script files have been archived in Zenodo (https://doi.org/10.5281/zenodo.6827798; Yeager et al. 2022).

Literature Cited

- Akaike, H. 1973. Information theory and an extension of the maximum likelihood principle. Pages 267–281 *in* B. N. Petriv and F. Csaki, eds. 2nd International Symposium on Information Theory. Akademia Kiado, Budapest.
- Anderson, E. 2008. The salesperson as outside agent or employee: a transaction cost analysis. Marketing Science 27:70–84.
- Anderson, R. P., and C. O. Handley Jr. 2002. Dwarfism in insular sloths: biogeography, selection, and evolutionary rate. Evolution 56:1045–1058.
- Arias, C. F., A. G. Munoz, C. D. Jiggins, J. Mavarez, E. Bermingham, and M. Linares. 2008. A hybrid zone provides evidence for incipient ecological speciation in *Heliconius* butterflies. Molecular Ecology 17: 4699–4712.
- Barton, N. H. 1979. The dynamics of hybrid zones. Heredity 43:341–359.
- Barton, N. H., and K. S. Gale. 1993. Genetic analysis of hybrid zones. Pages 13–45 in R. G. Harrison, ed. Hybrid zones and the evolutionary process. Oxford University Press, Oxford.
- Barton, N. H., and G. M. Hewitt. 1985. Analysis of hybrid zones. Annual Review of Ecology and Systematics 16:113–148.
- Benson, W. W. 1972. Natural selection for Müllerian mimicry in *Heliconius erato* in Costa Rica. Science 176:936–939.
- Blum, M. J. 2002. Rapid movement of a *Heliconius* hybrid zone: evidence for phase III of Wright's shifting balance theory? Evolution 56:1992–1998.
- 2008. Ecological and genetic associations across a *Heliconius* hybrid zone. Journal of Evolutionary Biology 21:330–341.
- Brower, A. V. 1994. Rapid morphological radiation and convergence among races of the butterfly *Heliconius erato* inferred from patterns of mitochondrial DNA evolution. Proceedings of the National Academy of Sciences of the USA 91:6491–6495.
- Brown, J. L., M. E. Maan, M. E. Cummings, and K. Summers. 2010. Evidence for selection on coloration in a Panamanian poison frog: a coalescent-based approach. Journal of Biogeography 37:891–901.
- Brumfield, R. T., R. W. Jernigan, D. B. McDonald, and M. J. Braun. 2001. Evolutionary implications of divergent clines in an avian (Manacus: Aves) hybrid zone. Evolution 55:2070–2087.
- Burnham, K. P., and D. R. Anderson. 2002. Model selection and multimodel inference. Springer, New York.
- Cummings, M. E., and L. R. Crothers. 2013. Interacting selection diversifies warning signals in a polytypic frog: an examination with the strawberry poison frog. Evolutionary Ecology 27:693–710.
- Daly, J., and C. W. Myers. 1967. Toxicity of Panamanian poison frogs (*Dendrobates*): some biological and chemical aspects. Science 156:970–973.
- Derryberry, E. P., G. E. Derryberry, J. M. Maley, and R. T. Brumfield. 2014. HZAR: hybrid zone analysis using an R software package. Molecular Ecology Resources 14:652–663.
- Dreher, C. E., M. E. Cummings, and H. Pröhl. 2015. An analysis of predator selection to affect aposematic coloration in a poison frog species. PLoS ONE 10:e0130571.
- Dugas, M. B., S. R. Halbrook, A. M. Killius, J. F. del Sol, and C. L. Richards-Zawacki. 2015. Colour and escape behaviour in polymorphic populations of an aposematic poison frog. Ethology 121:813–822.
- Dugas, M. B., and C. L. Richards-Zawacki. 2015. A captive breeding experiment reveals no evidence of reproductive isolation

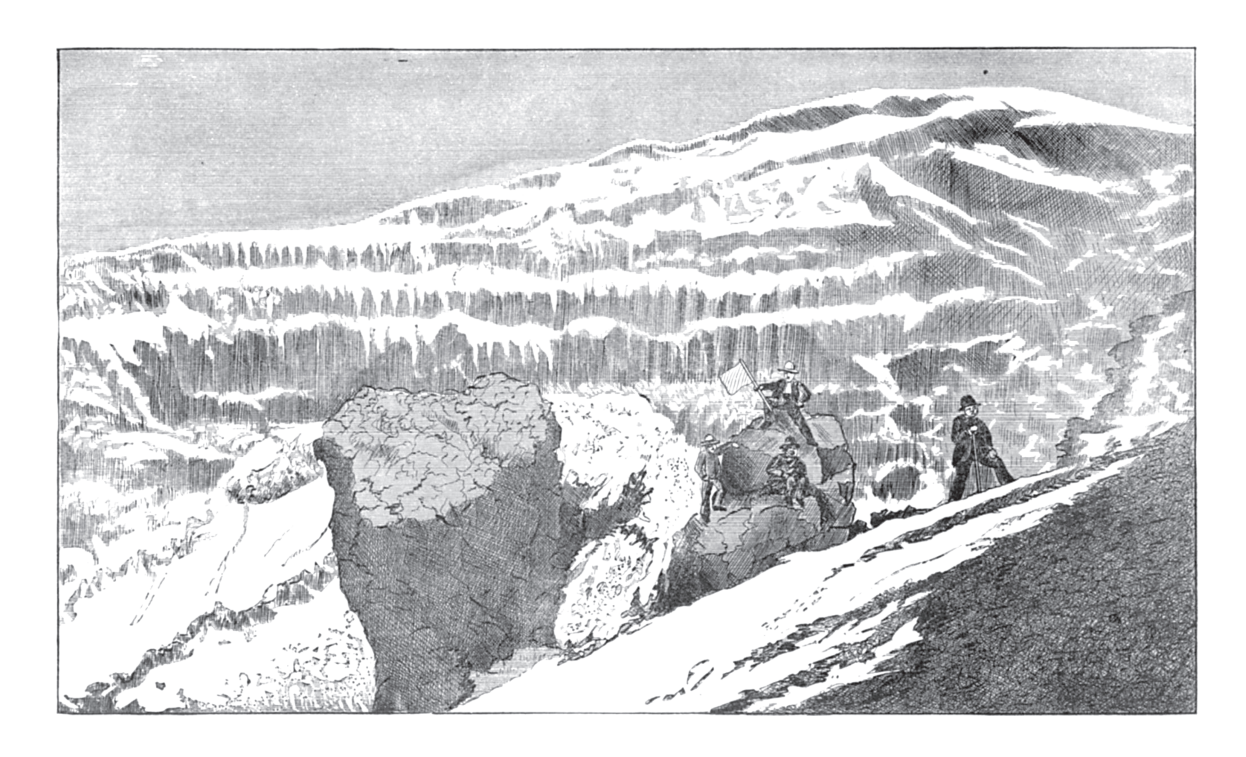
- among lineages of a polytypic poison frog. Biological Journal of the Linnean Society 116:52-62.
- Endler, J. A. 1977. Geographic variation, speciation, and clines. Princeton University Press, Princeton, NJ.
- Excoffier, L., G. Laval, and S. Schneider. 2005. Arlequin (version 3.0): an integrated software package for population genetics data analysis. Evolutionary Bioinformatics 1:47-50.
- Gehara, M., K. Summers, and J. L. Brown. 2013. Population expansion, isolation and selection: novel insights on the evolution of color diversity in the strawberry poison frog. Evolutionary Ecology 27:797-824.
- Glotzbecker, G. J., D. M. Walters, and M. J. Blum. 2016. Rapid movement and instability of an invasive hybrid swarm. Evolutionary Applications 9:741-755.
- Hagemann, S., and H. Pröhl. 2007. Mitochondrial paraphyly in a polymorphic poison frog species (Dendrobatidae; D. pumilio). Molecular Phylogenetics and Evolution 45:740-747.
- Hauswaldt, J. S., A. K. Ludewig, S. Hagemann, H. Pröhl, and M. Vences. 2009. Ten microsatellite loci for the strawberry poison frog (Oophaga pumilio). Conservation Genetics 10:1935-1937.
- Hauswaldt, J. S., A. K. Ludewig, M. Vences, and H. Pröhl. 2011. Widespread co-occurrence of divergent mitochondrial haplotype lineages in a Central American species of poison frog (Oophaga pumilio). Journal of Biogeography 38:711-726.
- Hegna, R. H., R. A. Saporito, and M. A. Donnelly. 2013. Not all colors are equal: predation and color polytypism in the aposematic poison frog Oophaga pumilio. Evolutionary Ecology 27:831-845.
- Jiggins, C. D., W. O. McMillan, P. King, and J. Mallet. 1997. The maintenance of species differences across a Heliconius hybrid zone. Heredity 79:495-505.
- Kapan, D. D. 2001. Three-butterfly system provides a field test of Müllerian mimicry. Nature 409:338-340.
- Knowles, L. L., and C. L. Richards. 2005. Importance of genetic drift during Pleistocene divergence as revealed by analyses of genomic variation. Molecular Ecology 14:4023-4032.
- Maan, M. E., and M. E. Cummings. 2008. Female preferences for aposematic signal components in a polymorphic poison frog. Evolution 62:2334-2345.
- Mallet, J. 1986. Hybrid zones of Heliconius butterflies in Panama and the stability and movement of warning colour clines. Heredity 56:191-202.
- Mallet, J., and N. H. Barton. 1989. Strong natural selection in a warning-color hybrid zone. Evolution 43:421-431.
- Mallet, J., N. Barton, G. Lamas, J. Santisteban, M. Muedas, and H. Eeley. 1990. Estimates of selection and gene flow from measures of cline width and linkage disequilibrium in Heliconius hybrid zones. Genetics 124:921-936.
- McMillan, W. O., C. D. Jiggins, and J. Mallet. 1997. What initiates speciation in passion-vine butterflies? Proceedings of the National Academy of Sciences of the USA 94:8628-8633.
- Nadeau, N. J., M. Ruiz, P. Salazar, B. Counterman, J. A. Medina, H. Ortiz-Zuazaga, A. Morrison, et al. 2014. Population genomics of parallel hybrid zones in the mimetic butterflies, H. melpomene and H. erato. Genome Research 24:1316-1333.
- Noonan, B. P., and A. A Comeault. 2009. The role of predator selection on polymorphic aposematic poison frogs. Biology Letters
- Pritchard, J. K., M. Stephens, and P. Donnelly. 2000. Inference of population structure using multilocus genotype data. Genetics 155:945-959.

- Pröhl, H., and O. Berke. 2001. Spatial distributions of male and female strawberry poison frogs and their relation to female reproductive resources. Oecologia 129:534-542.
- R Core Team. 2020. R: a language and environment for statistical computing. R Foundation for Statistical Computing, Vienna.
- Reynolds, R. G., and B. M. Fitzpatrick. 2007. Assortative mating in poison-dart frogs based on an ecologically important trait. Evolution 61:2253-2259.
- Richards-Zawacki, C. L., and M. E. Cummings. 2010. Intraspecific reproductive character displacement in a polymorphic poison dart frog, Dendrobates pumilio. Evolution 65:259-267.
- Richards-Zawacki, C. L., I. J. Wang, and K. Summers. 2012. Mate choice and the genetic basis for colour variation in a polymorphic dart frog: inferences from a wild pedigree. Molecular Ecology 21:3879-3892.
- Richards-Zawacki, C. L., J. Yeager, and H. P. S. Bart. 2013. No evidence for differential survival or predation between sympatric color morphs of an aposematic poison frog. Evolutionary Ecology 27: 783-795.
- Ringler, M., E. Ursprung, and W. Hödl. 2009. Site fidelity and patterns of short- and long-term movement in the brilliantthighed poison frog Allobates femoralis (Aromobatidae). Behavioral Ecology and Sociobiology 63:1281-1293.
- Rosser, N., K. K. Dasmahapatra, and J. Mallet. 2014. Stable Heliconius butterfly hybrid zones are correlated with a local rainfall peak at the edge of the Amazon basin. Evolution 68:3470-3484.
- Rudh, A., B. Rogell, and J. Höglund. 2007. Non-gradual variation in colour morphs of the strawberry poison frog Dendrobates pumilio: genetic and geographical isolation suggest a role for selection in maintaining polymorphism. Molecular Ecology 16:4284-4294.
- Runemark, A., M. Brydegaard, and E. I. Svensson. 2014. Does relaxed predation drive phenotypic divergence among insular populations? Journal of Evolutionary Biology 27:1676-1690.
- Runemark, A., B. Hansson, P. Pafilis, E. D. Valakos, and E. I. Svensson. 2010. Island biology and morphological divergence of the Skyros wall lizard Podarcis gaigeae: a combined role for local selection and genetic drift on color morph frequency divergence? BMC Evolutionary Biology 10:269.
- Saporito, R. A., T. F. Spande, H. M. Garraffo, and M. A. Donnelly. 2009. Arthropod alkaloids in poison frogs: a review of the "dietary hypothesis." Heterocycles 79:277-297.
- Seehausen, O., and D. Schluter. 2004. Male-male competition and nuptial-colour displacement as a diversifying force in Lake Victoria cichlid fishes. Proceedings of the Royal Society B 271:1345-
- Summers, K., E. Bermingham, L. Weight, S. McCafferty, and L. Dahistrom. 1997. Phenotypic and genetic divergence in three species of dart-poison frogs with contrasting parental behavior. Journal of Heredity 88:8-13.
- Summers, K., T. W. Cronin, and T. Kennedy. 2004. Cross-breeding of distinct color morphs of the strawberry poison frog (Dendrobates pumilio) from the Bocas del Toro Archipelago, Panama. Journal of Herpetology 38:1-8.
- Summers, K., R. Symula, M. Clough, and T. Cronin. 1999. Visual mate choice in poison frogs. Proceedings of the Royal Society B 266:2141-2145.
- Symula, R., R. Schulte, and K. Summers. 2001. Molecular phylogenetic evidence for a mimetic radiation in Peruvian poison frogs supports a Müllerian mimicry hypothesis. Proceedings of the Royal Society B 268:2415-2421.

- Szymura, J. M. 1993. Analysis of hybrid zones with *Bombina*. Pages 261–289 in R. G. Harrison. Hybrid zones and the evolutionary process. Oxford University Press, Oxford.
- Tazzyman, S. J., and Y. Iwasa. 2010. Sexual selection can increase the effect of random genetic drift—a quantitative genetic model of polymorphism in *Oophaga pumilio*, the strawberry poisondart frog. Evolution 64:1719–1728.
- Twomey, E., J. S. Vestergaard, and K. Summers. 2014. Reproductive isolation related to mimetic divergence in the poison frog *Ranitomeya imitator*. Nature Communications 5:4749.
- Twomey, E., J. S. Vestergaard, P. J. Venegas, and K. Summers. 2016. Mimetic divergence and the speciation continuum in the mimic poison frog *Ranitomeya imitator*. American Naturalist 187:205–223.
- Vestergaard, J. S., E. Twomey, R. Larsen, K. Summers, and R. Nielsen. 2015. Number of genes controlling a quantitative trait in a hybrid zone of the aposematic frog *Ranitomeya imitator*. Proceedings of the Royal Society B 282:20141950.
- Wang, I. J., and H. B. Shaffer. 2008. Rapid color evolution in an aposematic species: a phylogenetic analysis of color variation in the strikingly polymorphic strawberry poison-dart frog. Evolution 62:2742–2759.
- Wang, I. J., and K. Summers. 2009. Highly polymorphic microsatellite markers for the highly polymorphic strawberry poison-dart frog and some of its congeners. Conservation Genetics 10:2033–2036.
- Ward, J. L., M. J. Blum, D. M. Walters, B. A. Porter, N. Burkhead, and B. Freeman. 2012. Discordant introgression in a rapidly expanding hybrid swarm. Evolutionary Applications 5:380–392. Yang, Y., S. Blomenkamp, M. B. Dugas, C. L. Richards-Zawacki, and
- H. Pröhl. 2019a. Mate choice versus mate preference: inferences

- about color-assortative mating differ between field and lab assays of poison frog behavior. American Naturalist 193:598–607.
- Yang, Y., M. B. Dugas, H. J. Sudekum, S. N. Murphy, and C. L. Richards-Zawacki. 2018. Male-male aggression is unlikely to stabilize a poison frog polymorphism. Journal of Evolutionary Biology 31:457–468.
- Yang, Y., C. L. Richards-Zawacki, A. Devar, and M. B. Dugas. 2016. Poison frog color morphs express assortative mate preferences in allopatry but not sympatry. Evolution 70:2778–2788.
- Yang, Y., M. R. Servedio, and C. L. Richards-Zawacki. 2019b. Imprinting sets the stage for speciation. Nature 574:99–102.
- Yeager, J. 2015. Causes and consequences of warning color variation in a polytypic poison frog. PhD diss. Tulane University, New Orleans.
- Yeager, J., and J. B. Barnett. 2020. Ultraviolet components offer minimal contrast enhancement to an aposematic signal. Ecology and Evolution 10:13576–13582.
- ———. 2021. The influence of ultraviolet reflectance differs between conspicuous aposematic signals in neotropical butterflies and poison frogs. Ecology and Evolution 11:13633–13640.
- Yeager, J., J. L. Brown, V. Morales, M. Cummings, and K. Summers. 2012. Testing for selection on color and pattern in a mimetic radiation. Current Zoology 58:668–676.
- Yeager, J., G. E. Derryberry, M. J. Blum, and C. L. Richards-Zawacki. 2022. Data and code from: Selection and admixture in a polytypic aposematic frog. American Naturalist, Zenodo, https://doi.org/10.5281/zenodo.6827798.

Associate Editor: Rebecca C. Fuller Editor: Jennifer A. Lau



"Within the edge of the crater, looking across to the lava beds on S. E. side, forming the highest point of the summit." From "Ascent of the Volcano of Popocatepetl" by A. S. Packard (*The American Naturalist*, 1886, 20:109–123).